

50 3D Structural Optimization in Electromagnetics

R.H.W. Hoppe¹, S. Petrova², V. Schulz³

Introduction

We consider the optimal design and layout of high power electronic devices that are based on the pulse width modulation technique such as DC-AC converter modules used in applications as electric drives for high power electromotors. The design objective is to minimize power losses caused by eddy currents that build up in the device due to fast switching times and steep current ramps (cf., e.g., [BFS99, BHM01, DGH98]).

In mathematical terms this leads to a topology optimization problem with the electric conductivity of the material as the design parameter and the electric and the magnetic field as the state variables that are supposed to satisfy the quasistationary limit of Maxwell's equations. With the optimal design of mechanical structures described by continuum mechanical models being by now a well established discipline (cf., e.g., [BEN95] and the references therein), not much work has been done with regard to the optimization of systems whose operational behavior is governed by Maxwell's equations. Moreover, the use of modern discretization and numerical solution techniques such as multigrid and domain decomposition methods for optimization problems with PDE constraints is still in its infancy (cf., e.g., [HEI00, HPS01, MAS00]).

In this paper, we focus on an approach relying on a primal-dual Newton interior-point method for the discretized optimization problem where the discretization of the eddy currents equations is taken care of by curl-conforming edge elements. Domain decomposition methods on nonmatching grids can be used for the numerical solution of the discretized field equations which is an integral part of the optimization routine featuring logarithmic barrier functions and simultaneous sequential quadratic programming.

The topology optimization problem

We consider a DC-AC converter module consisting of specific semiconductor devices such as IGBTs (Insulated Gate Bipolar Transistors) and GTOs (Gate Turn-Off Thyristors) that are interconnected and linked to the high power source as well as the load by copper made bus bars (cf. Figure 1).

Each bus bar contains a certain number of ports where currents are either supplied to or taken off the bar. The IGBTs and GTOs serve as valves for the currents which can be in the range of several kA. During operation of the module, electromagnetic fields \mathbf{E} and \mathbf{H} are generated that can be described by the eddy currents equations

$$\frac{\partial \mathbf{B}}{\partial t} + \mathbf{curl} \mathbf{E} = \mathbf{0} \quad , \quad \mathbf{div} \mathbf{B} = 0 \quad , \quad \mathbf{curl} \mathbf{H} = \mathbf{J} \quad , \quad (1)$$

¹Institute of Mathematics , University of Augsburg, D-86159 Augsburg, Germany

²Institute of Mathematics , University of Augsburg, D-86159 Augsburg, Germany ; on leave from the Bulgarian Academy of Sciences, Sofia, Bulgaria

³Weierstrass Institute Berlin, D-10117 Berlin, Germany

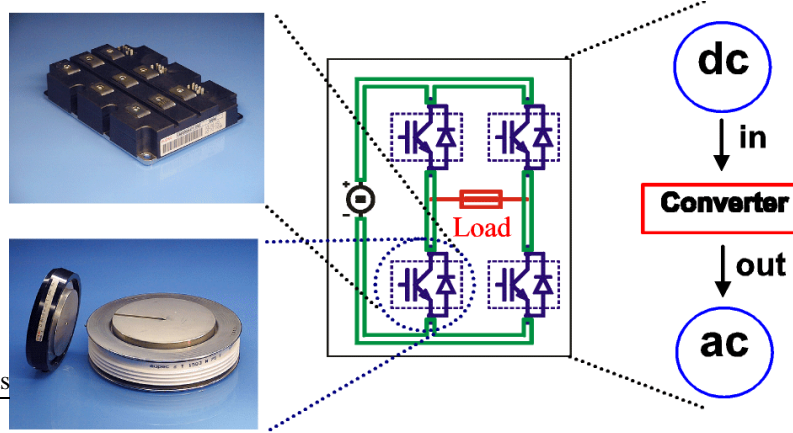


Figure 1: DC-AC converter module

$$\mathbf{B} = \mu \mathbf{H} , \quad \mathbf{J} = \sigma \mathbf{E} . \quad (2)$$

where \mathbf{B} and \mathbf{J} stand for the magnetic induction and the current density, μ denotes the magnetic permeability, and σ is the electric conductivity.

Considering a module $\Omega = \cup_{\nu=1}^N \Omega_{\nu}$ with N bars Ω_{ν} , $1 \leq \nu \leq N$, each bar containing N_{ν} ports $\Gamma_{\nu\alpha}$, $1 \leq \alpha \leq N_{\nu}$, and introducing a scalar electric potential φ and a magnetic vector potential \mathbf{A} according to

$$\mathbf{E} = -\text{grad } \varphi - \frac{\partial \mathbf{A}}{\partial t} , \quad \mathbf{B} = \text{curl } \mathbf{A}$$

we are led to the following coupled system of PDEs

$$\text{div} (\sigma \text{grad } \varphi) = 0 \quad \text{in } \Omega , \quad (3)$$

$$\sigma \mathbf{n} \cdot \text{grad } \varphi = \begin{cases} -I_{\nu\alpha}(t) & \text{on } \Gamma_{\nu\alpha} \\ 0 & \text{else} \end{cases} \quad (4)$$

$$\sigma \frac{\partial \mathbf{A}}{\partial t} + \text{curl } \mu^{-1} \text{curl } \mathbf{A} = \begin{cases} -\sigma \text{grad } \varphi & \text{in } \Omega \\ 0 & \text{in } \mathbf{R}^3 \setminus \Omega \end{cases} \quad (5)$$

with appropriate initial and boundary conditions.

Note that in (4) we refer to $I_{\nu\alpha}$ as the fluxes associated with the ports $\Gamma_{\nu\alpha}$ satisfying $\sum_{\nu=1}^N \sum_{\alpha=1}^{N_{\nu}} I_{\nu\alpha} = 0$.

The total inductivity caused by the eddy currents can be described by the functional

$$L(\sigma, \varphi, \mathbf{A}) := \left(\sum_{\nu, \alpha} \sum_{\mu, \beta} \int_0^T |L_{\nu\alpha, \mu\beta}(t)|^2 dt \right)^{1/2} . \quad (6)$$

Here, $L_{\nu\alpha,\mu\beta}(t)$ are the generalized transient inductivity coefficients

$$L_{\nu\alpha,\mu\beta}(t) := \sigma^{-1} \int_{\Omega_\nu} \mathbf{J}_{\nu\alpha}(x) \cdot \mathbf{S}(t) \mathbf{J}_{\mu\beta}(x) dx$$

where $\mathbf{J}_{\nu\alpha}$ denotes the current density generated by $I_{\nu\alpha}$ at the port $\Gamma_{\nu\alpha}$ of the bus bar Ω_ν and $\mathbf{S}(\cdot)$ is the solution operator associated with (5).

The design objective is to distribute the material in terms of the electric conductivity σ as the design parameter in such a way that the total inductivity is minimized

$$\inf_{\sigma, \varphi, \mathbf{A}} L(\sigma, \varphi, \mathbf{A}) \quad (7)$$

subject to the equality constraints

$$\varphi \text{ and } \mathbf{A} \text{ satisfy the state equations (3),(4),(5),} \quad (8)$$

$$\int_{\Omega} \sigma dx = C \quad (9)$$

and the inequality constraints

$$\sigma_{min} \leq \sigma \leq \sigma_{max} \quad (10)$$

where $0 < \sigma_{min} \ll 1$ and σ_{max} refers to the conductivity of copper.

Note that (10) represents relaxed constraints on the design parameter, since allowing only $\sigma = \sigma_{max}$ or $\sigma = \sigma_{min}$ would lead to an ill-posed optimization problem. In practice, we scale the conductivity by means of

$$\eta(\sigma) = \left(\frac{\sigma - \sigma_{min} + \varepsilon}{\sigma_{max} - \sigma_{min}} \right)^m, \quad 0 < \varepsilon \ll 1 \quad (11)$$

with an appropriately chosen $m \geq 1$.

The primal-dual Newton interior-point method

The discretization of the state equations (3),(4),(5) is performed as follows: For the interior-exterior domain problem (5) we use a domain decomposition approach on nonmatching grids featuring individual edge element discretizations of the interior and exterior domain problems with respect to simplicial triangulations $\mathcal{T}_h^{(I)}$ and $\mathcal{T}_h^{(E)}$ whereas the discretization in time is done by the backward Euler scheme. Moreover, the elliptic boundary value problem (3),(4) is discretized by means of nonconforming Crouzeix-Raviart elements. The electric conductivity σ serving as the design parameter is discretized by elementwise constants, i.e., $\vec{\sigma}_h = (\sigma_h^{(1)}, \dots, \sigma_h^{(m_h)})^T$, $m_h := \text{card } \mathcal{T}_h^{(I)}$. Comprising the discrete state variables $\vec{\varphi}_h$ and $\vec{\mathbf{A}}_h$ to a vector $\vec{\mathbf{u}}_h = (\vec{\varphi}_h, \vec{\mathbf{A}}_h)^T$, the discretized state equations can be stated in compact form

$$A_h(\vec{\sigma}_h) \vec{\mathbf{u}}_h = \vec{b}_h. \quad (12)$$

If we further denote by $L_h(\vec{\sigma}_h, \vec{\varphi}_h, \vec{\mathbf{A}}_h)$ the discretized objective functional, the topology optimization problem in the discrete regime reads as follows:

$$\min_{\vec{\sigma}_h, \vec{\varphi}_h, \vec{\mathbf{A}}_h} L_h(\vec{\sigma}_h, \vec{\varphi}_h, \vec{\mathbf{A}}_h) \quad (13)$$

subject to the constraints

$$\vec{\mathbf{u}}_h = (\vec{\varphi}_h, \vec{\mathbf{A}}_h)^T \text{ satisfies (12) ,} \quad (14)$$

$$g_h(\vec{\sigma}_h) := \sum_{i=1}^{m_h} |K_i| \sigma_h^{(i)} = C , \quad (15)$$

$$\sigma_{\min} \vec{\mathbf{e}}_h \leq \vec{\sigma}_h \leq \sigma_{\max} \vec{\mathbf{e}}_h , \quad (16)$$

where $K_i \in \mathcal{T}_h^{(I)}$, $1 \leq i \leq m_h$, and $\vec{\mathbf{e}}_h := (1, \dots, 1)^T$.

Among the most efficient numerical solution techniques for constrained optimization problems like (13)-(16) are primal-dual Newton interior-point methods (cf., e.g., [ETT96, FOG98, GOW98]). The idea is to take care of the inequality constraints (16) by parametrized logarithmic barrier functions

$$B_h^p(\vec{\sigma}_h, \vec{\mathbf{u}}_h) := L_h(\vec{\sigma}_h, \vec{\varphi}_h, \vec{\mathbf{A}}_h) - p [\log(\vec{\sigma}_h - \sigma_{\min} \vec{\mathbf{e}}_h) + \log(\sigma_{\max} \vec{\mathbf{e}}_h - \vec{\sigma}_h)]$$

and to couple the equality constraints (14),(15) by Lagrangian multipliers. This gives rise to the saddle point problem

$$\min_{\vec{\sigma}_h, \vec{\mathbf{u}}_h} \max_{\vec{\lambda}_h, \eta_h} \mathcal{L}_h^{(p)}(\vec{\sigma}_h, \vec{\mathbf{u}}_h, \vec{\lambda}_h, \eta_h) \quad (17)$$

for the Lagrangian

$$\mathcal{L}_h^{(p)}(\vec{\sigma}_h, \vec{\mathbf{u}}_h, \vec{\lambda}_h, \eta_h) := B_h^p(\vec{\sigma}_h, \vec{\mathbf{u}}_h) + \vec{\lambda}_h^T (A_h(\vec{\sigma}_h) \vec{\mathbf{u}}_h - \vec{\mathbf{b}}_h) + \eta_h (g_h(\vec{\sigma}_h) - C) .$$

For the solution of the above primal-dual interior-point approach we use simultaneous sequential quadratic programming in the sense that Newton's method is applied to the Karush-Kuhn-Tucker conditions associated with (13). Denoting the Newton increments by $\Delta \vec{\Psi}_h := (\Delta \vec{\mathbf{u}}_h, \Delta \vec{\lambda}_h, \Delta \vec{\sigma}_h, \Delta \eta_h)^T$, this gives rise to a linear system

$$\mathcal{K}_h \Delta \vec{\Psi}_h = \vec{\mathbf{d}}_h \quad (18)$$

which is solved iteratively by right transforming iterations

$$\Delta \vec{\Psi}_h^{\nu+1} = \Delta \vec{\Psi}_h^\nu + \mathcal{K}_h^R (\mathcal{M}_h^{(1)})^{-1} (\vec{\mathbf{d}}_h - \mathcal{K}_h \Delta \vec{\Psi}_h^\nu) \quad (19)$$

based on a regular splitting $\mathcal{K}_h \mathcal{K}_h^R = \mathcal{M}_h^{(1)} - \mathcal{M}_h^{(2)}$ involving an appropriately chosen right transform \mathcal{K}_h^R . The new iterate $\vec{\Psi}_h^{(\text{new})} := (\vec{\mathbf{u}}_h^{(\text{new})}, \vec{\lambda}_h^{(\text{new})}, \vec{\sigma}_h^{(\text{new})}, \eta_h^{(\text{new})})^T$ is then obtained by a line search

$$\vec{\Psi}_{h,i}^{(\text{new})} = \vec{\Psi}_{h,i}^{(\text{old})} + s_i (\Delta \vec{\Psi}_h)_i , \quad 1 \leq i \leq 4 , \quad (20)$$

where the steplengths are tested by means of a hierarchy of merit functions. We refer to [HPS00, HPS01] for details.

Domain decomposition on nonmatching grids

The simultaneous sequential quadratic programming approach being integral part of the primal-dual Newton interior-point method, described in the previous section, requires an iterative solver of the discretized state equations. In this section, we briefly sketch a domain decomposition technique on nonmatching grids for the implicitly in time discretized equation (5) with respect to a nonoverlapping geometrically conforming decomposition $\bar{\Omega} = \bigcup_{i=1}^n \bar{\Omega}_i$ with skeleton $S = \bigcup_{i \neq j} \Gamma_{ij}$, $\Gamma_{ij} := \bar{\Omega}_i \cap \bar{\Omega}_j$. In particular, we consider individual simplicial triangulations $\mathcal{T}_h^{(i)}$ of the subdomains and discretize the subdomain problems by the lowest order curl-conforming edge elements $Nd_1(K) := \{ \mathbf{q} = \mathbf{a} + \mathbf{b} \wedge \mathbf{x} \mid \mathbf{a}, \mathbf{b} \in \mathbf{R}^3 \}$, $K \in \mathcal{T}_h^{(i)}$ with the degrees of freedom given by the moments of the tangential components with respect to the edges of K (cf. [NED80]). Since nonconforming nodal points may occur on the interfaces $\Gamma_{ij} \subset S$, continuity of the tangential components across the interfaces is not guaranteed requiring weak continuity constraints on the skeleton in order to achieve consistency of the global approximation. This is taken care of by appropriately chosen Lagrangian multipliers living in multiplier spaces $\mathbf{M}_h(\Gamma_{ij})$, $\Gamma_{ij} \subset S$ (for the construction of $\mathbf{M}_h(\Gamma_{ij})$ we refer to [HOP99]). Introducing the product spaces

$$\mathbf{V}_h(\Omega) := \prod_{i=1}^n Nd_1(\Omega_i, \mathcal{T}_h^{(i)}) \quad , \quad \mathbf{M}_h(S) := \prod_{\Gamma_{ij} \subset S} \mathbf{M}_h(\Gamma_{ij}) \quad ,$$

where $Nd_1(\Omega_i, \mathcal{T}_h^{(i)})$ are the edge element spaces associated with the subdomains, the domain decomposition approach leads to the discrete saddle point problem:

Find $(\mathbf{u}_h, \lambda_h) \in \mathbf{V}_h(\Omega) \times \mathbf{M}_h(S)$ such that

$$a_h(\mathbf{u}_h, \mathbf{v}_h) + b_h(\mathbf{v}_h, \lambda_h) = \ell(\mathbf{v}_h) \quad , \quad \mathbf{v}_h \in \mathbf{V}_h(\Omega) \quad , \quad (21)$$

$$b_h(\mathbf{u}_h, \mu_h) = 0 \quad , \quad \mu_h \in \mathbf{M}_h(S) \quad . \quad (22)$$

Here, the bilinear form $a_h : \mathbf{V}_h(\Omega) \times \mathbf{V}_h(\Omega) \rightarrow \mathbf{R}$ and the functional $\ell_h : \mathbf{V}_h(\Omega) \rightarrow \mathbf{R}$ are given by

$$a_h(\mathbf{u}_h, \mathbf{v}_h) := \sum_{i=1}^n \int_{\Omega_i} [\Delta t \mu^{-1} \mathbf{curl} \mathbf{u}_h \cdot \mathbf{curl} \mathbf{v}_h + \sigma \mathbf{u}_h \cdot \mathbf{v}_h] dx \quad ,$$

$$\ell_h(\mathbf{v}_h) := \int_{\Omega} \sigma [\mathbf{u}_h^{m-1} \cdot \mathbf{v}_h - \Delta t \mathbf{grad} \varphi_h^m \cdot \mathbf{v}_h] dx \quad ,$$

where \mathbf{u}_h^{m-1} and φ_h^m refer to the FE approximations of the magnetic vector potential and the scalar electric potential at time t_{m-1} and t_m , respectively, and $\Delta t := t_m - t_{m-1}$.

Moreover, the bilinear form $b_h : \mathbf{V}_h(\Omega) \times \mathbf{M}_h(S) \rightarrow \mathbf{R}$ realizing the weak continuity of the tangential components across the interfaces is chosen as follows

$$b_h(\mathbf{v}_h, \vec{\mu}_h) := \sum_{\Gamma_{ij} \subset S} \int_{\Gamma_{ij}} \vec{\mu}_h \cdot [\mathbf{n} \wedge \mathbf{v}_h] |_{\Gamma_{ij}} ds$$

with $[\mathbf{n} \wedge \mathbf{v}_h] |_{\Gamma_{ij}}$ denoting the jump of $\mathbf{n} \wedge \mathbf{v}_h$ across the interface $\Gamma_{ij} \subset S$.

It can be shown that $a_h(\cdot, \cdot)$ is elliptic on the kernel of the operator associated with $b_h(\cdot, \cdot)$ and

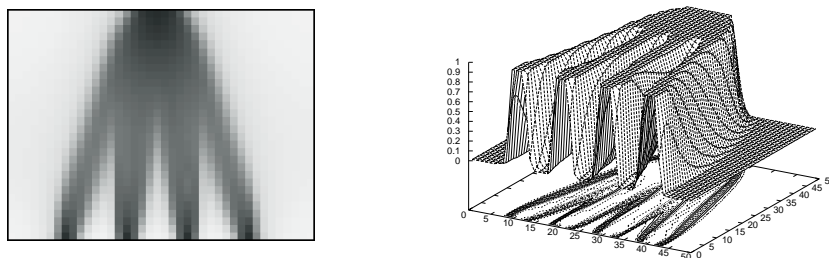


Figure 2: Material distribution (5 ports)

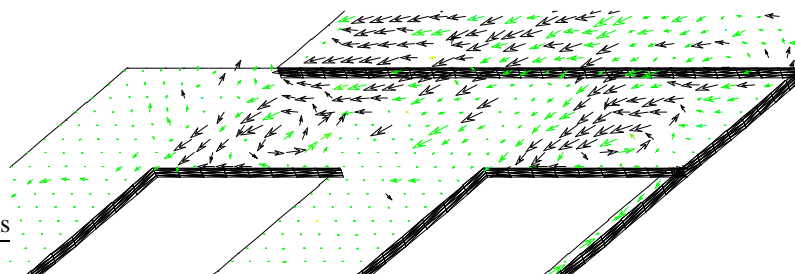


Figure 3: Magnetic induction between two ports (zoom)

that $b_h(\cdot, \cdot)$ satisfies an LBB-condition (cf. [HOP99]). The numerical solution of (21),(22) is done by preconditioned Richardson-type iterations with a multilevel preconditioner and features an additional defect correction in subspaces of irrotational vector fields that takes care of the nontrivial kernel of the discrete curl-operator. We refer to [HOP00] for details (cf. also [BBM99] for a related approach). Grid adaptation strategies based on efficient and reliable residual-type a posteriori error estimators can be performed along the lines of [BHH00]).

Numerical results

The primal-dual Newton interior-point method has been tested in 2D with the total amount of dissipated electric energy to be minimized and an optimal design has been computed in 3D for an individual bus bar by using the techniques described in the previous sections. The numerical simulation provides a material distribution that can be visualized by grey-scales ranging from black ($\sigma = \sigma_{max}$) to white ($\sigma = \sigma_{min}$) and by corresponding height profiles. Figure 2 displays the material distribution for a 2D test case (bus bar with 5 ports).

We observe a sharp resolution of the interface “material - no material”. The performance of the primal-dual Newton interior-point method depends on the number of ports and the parameter m in (11) (for details see [HPS00]).

For an individual 3D bus bar, Figure 3 shows a visualization of the computed magnetic induction \mathbf{B} for the final design in a vicinity between two ports. One clearly recognizes the effect of the topology optimization (holes close to the ports) on the distribution of the magnetic

induction (for a more detailed documentation we refer to [BHM01]).

Acknowledgments. The work has been supported by grants from the Federal Ministry for Education and Research (BMBF) under Grant No. 03HO7AU1-8 and Grant No. 03HOM3A1 and from the German National Science Foundation (DFG) under Grant No. HO877/4-1 and Grant No. HO877/5-1. The second author is indebted to the Alexander-von-Humboldt Foundation for an AvH-Fellowship.

References

- [BDH99]R. Beck, P. Deuffhard, R. Hiptmair, R.H.W. Hoppe, and B. Wohlmuth, “Adaptive multilevel methods for edge element discretizations of Maxwell’s equations”, *Surveys of Math. in Industry*, Vol. **8**, pp. 271–312, (1999).
- [BHH00]R. Beck, R. Hiptmair, R.H.W. Hoppe, and B. Wohlmuth, “Residual based a posteriori error estimators for eddy current computation”, to appear in *M²AN Math. Modelling and Numer. Anal.*, (2000).
- [BBM99]F. Ben Belgacem, A. Buffa, and Y. Maday, “The mortar finite element method for 3D Maxwell equations: First results”, Report 99023, Laboratoire d’Analyse Numérique, Université Pierre et Marie Curie, Paris, (1999).
- [BEN95]M.P. Bendsøe, “Optimization of Structural Topology, Shape, and Material”, Springer, Berlin-Heidelberg-New York, 1995.
- [BFS99]P. Böhm, E. Falck, J. Sigg, and G. Wachutka, “Numerical analysis of distributed inductive parasitics in high power bus bars”, In: *High Performance Scientific and Engineering Computing. Proc. ”Int. FORTWIHR-Symposium”*, Munich, March 1998 (Bungartz, H., Durst, F., and Zenger, Chr.; eds.), pp. 397-404, *Lecture Notes in Computational Science and Engineering*, Vol. **8**, Springer, Berlin-Heidelberg-New York, 1999
- [BHM01]P. Böhm, R.H.W. Hoppe, G. Mazurkevitch, S. Petrova, G. Wachutka, and E. Wolfgang, “Optimal design of high power electronic devices by topology optimization”, to appear in: *Mathematik - Schlüsseltechnologie für die Zukunft. Verbundprojekte zwischen Mathematik und Industrie*, Springer, Berlin-Heidelberg-New York, (2001).
- [DGH98]St. Dürndorfer, V. Gradinaru, R.H.W. Hoppe, E.-R. König, G. Schrag, and G. Wachutka, “Numerical simulation of microstructured semiconductor devices, transducers, and systems”, In: *High Performance Scientific and Engineering Computing. Proc. ”Int. FORTWIHR-Symposium”*, Munich, March 1998 (Bungartz, H., Durst, F., and Zenger, Chr.; eds.), pp. 309–323, *Lecture Notes in Computational Science and Engineering*, Vol. **8**, Springer, Berlin-Heidelberg-New York, (1999).
- [ETT96]A.S. El-Bakry, R.A. Tapia, T. Tsuchiya, and Y. Zhang, “On the formulation of the Newton interior-point method for nonlinear programming”, *Journal of Optimization Theory and Applications*, **89**, 507-541, (1996).
- [FOG98]A. Forsgen and Ph. Gill, “Primal-dual interior methods for nonconvex nonlinear programming”, *SIAM J. Optimization* **8**, 1132-1152, (1998).
- [GOW98]D.M. Gay, M.L. Overton, and M.H. Wright, “A primal-dual interior method for nonconvex nonlinear programming”, In: *Advances in Nonlinear Programming* (Yuan, Y.; ed.), pp. 31-56, Kluwer, Dordrecht, (1998)

- [HEI00]M. Heinkenschloss, “Time-domain decomposition iterative methods for the solution of parabolic linear-quadratic optimal control problems”, Techn. Rep., Department of Comput. and Appl. Math., Rice University, Houston, (2000).
- [HOP99]R.H.W. Hoppe, “Mortar edge elements in \mathbf{R}^3 ”, East-West J. Numer. Anal., Vol. 7, 159–173, (1999).
- [HOP00]R.H.W. Hoppe, “Adaptive mortar edge elements in the computation of eddy currents”, In: Proc. Conf. ”Analysis and Approximation of Boundary Value Problems”, Jyväskylä (Finland), October 1998 (Neittaanmäki, P. et al.; eds.), (2000).
- [HPS00]R.H.W. Hoppe, S. Petrova, and V. Schulz, “A primal-dual Newton-type interior-point method for topology optimization”, to appear in Journal of Optimization: Theory and Applications, 2002
- [HPS01]R.H.W. Hoppe, S. Petrova, and V. Schulz, “Topology optimization of high power electronic devices”, to appear in Proc. Oberwolfach Conf. ”Optimal Control of Complex Dynamical Structures”, June 4-10, 2000 (Hoffmann, K.-H. and Leugering, G.; eds.), Birkhäuser, Basel, 2001
- [MAS00]B. Maar and V. Schulz, “Interior point multigrid methods for topology optimization”, Structural Optimization **19**, 214-224, (2000).
- [NED80]J.-C. Nédélec, “Mixed finite elements in \mathbf{R}^3 ”, Numer. Math. **35**, 315-341, (1980).